行政院國家科學委員會專題研究計畫 期中進度報告

以分子電腦模擬探討PTT(聚對苯二甲酸丙二酯)纖維之結構與性質之關係(2/3)
期中進度報告(精簡版)

計 畫 類 別 ：個別型
計 畫 編 號 ：NSC 95-2221-E-002-290-
執 行 期 間 ：95 年 08 月 01 日至 96 年 07 月 31 日
執 行 單 位 ：國立臺灣大學化學工程學系暨研究所

計 畫 主 持 人：林祥泰

處 理 方 式 ：期中報告不提供公開查詢

中 華 民 國 96 年 05 月 30 日

Progress Report for

Atomistic Molecular Dynamics Simulations for the Morphology and Property Relationship of Poly(Trimethylene Terephthalate) fiber

Shiang-Tai Lin

Department of Chemical Engineering, National Taiwan University

Abstract

Recent discovery of a low-cost production of poly (trimethylene terephthalate) (PTT) has led to a renewed interest in its study. In particular, the morphology of the polymer molecules is the key to understanding the variation of the properties of PTT fibers under different processing conditions. In this 3-year project, we propose to use molecular dynamic simulations to determine both the morphology and properties of PTT at the atomic level. In the past year (year 2), we have determined various physical and mechanical properties of PTT and observed the temperature induced crystallization phenomena in our simulation. Specific work that has been accomplished includes

1. Determination of the mechanical properties such as the Young's modulus of PTT.
2. Determination of the glass transition temperature (T_g) and melting temperature (T_m) of PTT.
3. Microstructure analysis of PTT during crystallization from its melt.

Our atomistic molecular dynamic simulations reveal the formation and growth of highly oriented but loosely packed clusters upon quenching a melted semi-rigid polymer, poly(trimethylene terephthalate). The formation of the precursors is found to be rapid and may play an important role as an incubator for crystal nuclei formation. We find that the formation of such nucleus precursors may take place as soon as the polymer enters a metastable state. The growth of the precursor is found to be quite rapid, with the Avrami rate constant being, 8.16×10^7 $s^{-0.9}$. These results provide fruitful insights to the molecular mechanism of polymer crystallization.

Introduction

In the first year of this three-year project, we have successfully used molecular dynamics simulations to determine the structure, energetic, and vibrational (Infrared) properties of PTT both in the crystalline and in the amorphous state. Based on this foundation, we have now moved forward to study the crystallization process of PTT under thermal (cooling) and stress (drawing) treatments. Our focus in the past (second) year was to investigate the mechanism of PTT crystallization whiling cooling it from its melt.

In classical theory of nucleation, the crystallization of a material when cooled to a temperature below its melting point is generally recognized to be a two-stage process. In the stage of primary nucleation, crystal nuclei (clusters comprising ordered molecules) appear and re-dissolve via molecular collisions until the size of a nucleus reaches some critical value, above which the nuclei are thermodynamically stable. The subsequent growth of the critical nuclei follows kinetic mechanism and is classified as secondary nucleation. Complicated by additional constraints in topological connectivity, the crystallization in polymers presents remarkable differences both in the nucleation and in the growth periods when compared to that in small molecules. While extensive experimental [1-4] and theoretical [5-7] efforts are made to verify and explain the molecular mechanism in the growth of nuclei in polymeric materials, the primary stage of polymer crystallization is less well understood. Recent works [8-14] show that there exist nucleus precursors prior to the formation of crystal nuclei. While such existence of nucleus precursors is criticized by some researchers [15-17], some believed that the precursors may be the reason for memory effects in polymeric materials [18]. Simulation work of Gee et al. [19] provided an unambiguous evidence of precursor formation as polymer melts are deep quenched into the unstable region where spinodal decomposition starts.

Our recent atomistic molecular dynamic simulations reveal the formation and growth of highly oriented but loosely packed clusters upon quenching a melted poly(trimethylene terephthalate). Unlike the work of Gee et al., here we show that such precursors may occur much earlier as soon as the polymer enters the metastable region. The formation of the precursors is found to be rapid and may play an important role as an incubator for crystal nuclei formation.

Simulation Details

Molecular dynamics simulations are performed to study the precrystallization process of poly(trimethylene terephthalate), PTT (whose chemical structure is shown in Fig. 1). PTT, a member of aromatic polyesters, exhibits outstanding elastic recovery and resiliency properties over its homologous sisters PET and PBT. The molecular models of PTT are prepared using commercial package Cerius2 [20]. Each

model contains 4 chains of PTT molecules, each having a degree of polymerization of 27 (i.e., 5568g/mol. Note that the entanglement molecular weight of PTT was determined to be 4900 to 5000 g/mol. [21, 22]) Thus each unit cell contains 108 repeating units of PTT, or, equivalently, 2708 atoms. Note that the use of relative small system sizes in our simulations effectively prevents fluctuations of long wavelengths within the system, i.e., no spinodal decomposition is possible. The computer code LAMMPS [23] is used for all subsequent molecular dynamic simulations. A series of expansion and compression steps were applied to the initial structures in order to obtain equilibrium samples at 600K (which is above the melting temperature T_m). The equilibrated sample is then cooled to 50 K at a rate of 1 K/ps. At each 50 K interval during the quenching process, simulation samples are taken and subjected to long (up to 7 ns), constant temperature and pressure simulations for the nucleation analysis. The particle-particle-particle mesh Ewald technique [24] is used for the long range electrostatic interactions. Nose-Hoover thermostat is used for temperature control. The integration time step used is 0.5 to 1 fs.

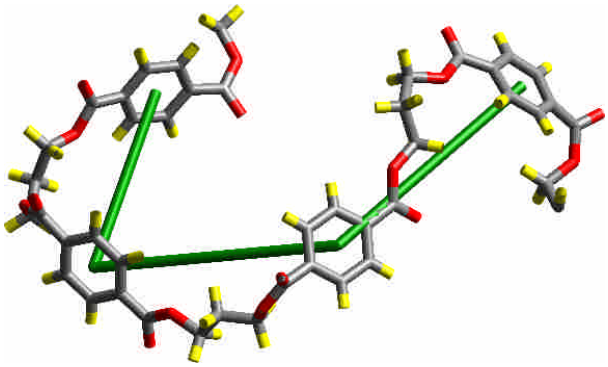

Figure 1. A fragment (4 repeating units) of the PTT chain. Carbon atoms are shown in grey, oxygen in red, and hydrogen in yellow. The green cylinders connecting the centers of adjacent aromatic rings are taken as elementary segments in the precursor analysis.

Results and Discussion

In the following the result of our simulation work is organized in three parts: (1) the mechanical property of PTT, (2) the melting and glass transition temperature of PTT, (3) the formation of nucleus precursor of PTT while quenching from the melted state. The first two parts are served as a validation of the force field used in our simulation.

1. Mechanical property (Yong's modulus) of amorphous PTT

The elastic constant of PTT is determined from the slope of the stress-strain curves. The amorphous PTT sample is stretched in some direction (x, y, or z axis) at 3 different deformation rates (10^{11} s^{-1} to 10^{9} s^{-1}). The results are illustrated in Fig. 2.

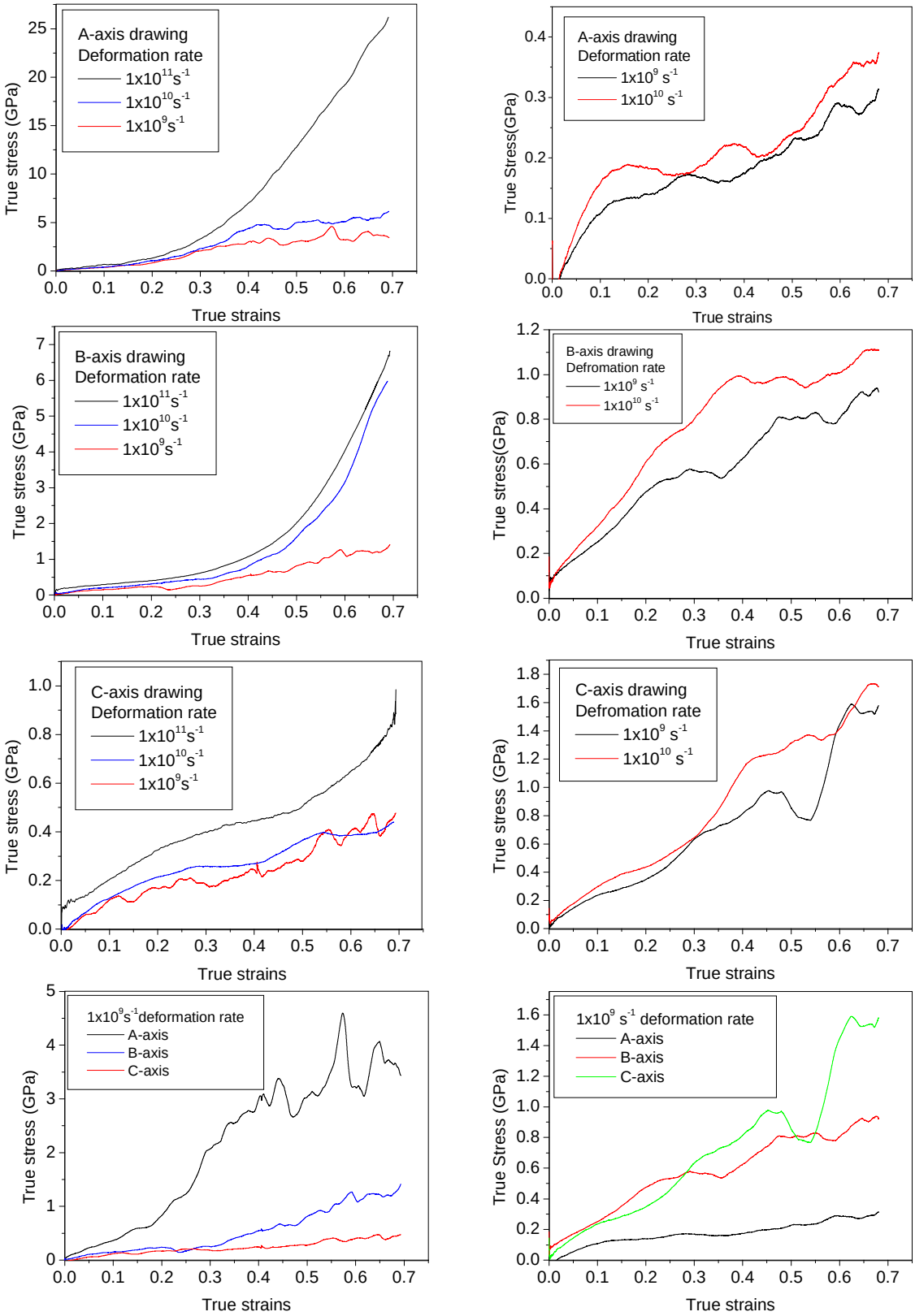

Fig. 2 The stress strain-curve of PTT from three axes at different deformation rates.

Table 1 summarizes the calculated result of Young's modulus. The average value from simulation is 3.35±0.21 GPa. This is in good agreement with that from experiments, 2.3~2.8 GPa [25-27].

Table 1 The Calculated Result of Young's Modulus Value.

PTT sample	Deformation rate (s^{-1})	E_a	E_b	E_c	<E>
54-4-17	1×10^{10}	6.48	2.88	0.73	3.36
54-4-18	1×10^{9}	3.88	3.59	5.42	4.30
	1×10^{10}	5.04	1.98	7.13	4.72
18-12-4	1×10^{9}	4.40	3.24	4.58	4.07
	1×10^{10}	5.53	4.91	2.02	4.15
18-12-6	1×10^{9}	2.98	1.98	4.05	3.00
	1×10^{10}	4.64	2.96	2.24	3.28

2. Melting and glass transition temperatures of PTT

The melting temperature (T_m), below which crystallization driven by thermodynamics may occur, and glass transition temperature (T_g), below which crystallization may cease due to the lack of sufficient molecular mobility, are determined by examination of the variation of density upon cooling and heating at a rate of 1K/1ps. Hysteresis in the density change is observed as shown in Fig. 3. Upon cooling we observe a discontinuous change in density at 500 ~ 550 K (T_m, experimental value is 499~503 K [1, 25, 28]) and a change of slope at 350 K. Upon heating we observe a change of slope in the density at about 400 K. These results suggest that the T_g is about 375 K (experimental value is 315~348 K [3, 25]). The overestimation of T_g from simulation may be a result of the rapid cooling rate used here.

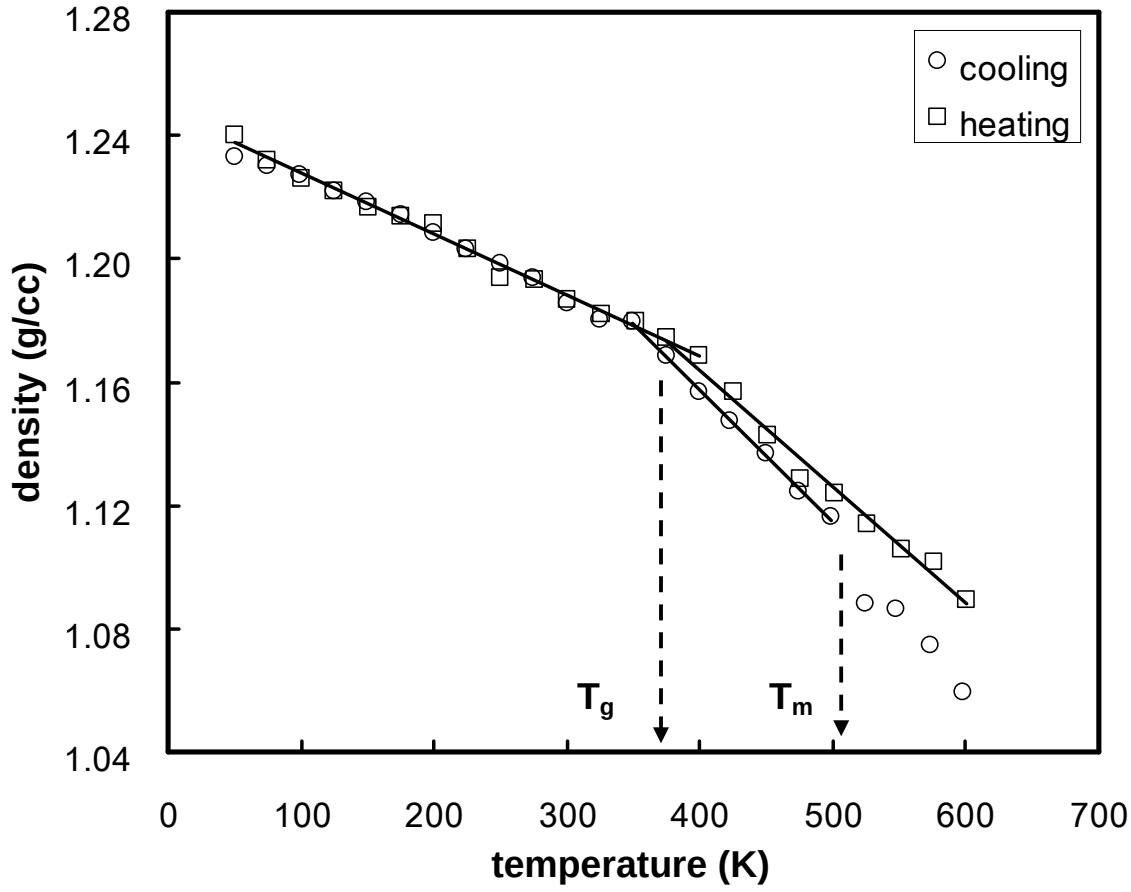

Figure 3. The density variation of PTT upon cooling and heating.

3. Formation of pre-crystal nuclei whiling cooling PTT from its melt

3.1 Definition of nucleus precursor

To detect and quantify any structural development, we define the nucleus precursors in the system as follows. (1) A segment of PTT is defined to be the vector pointing from the center of an aromatic ring to the next aromatic ring on the same polymer chain (green cylinders in Fig. 1). (2) Adjacent segments are defined as those whose distance between center of mass fall within 9 Å. [note the lengths of a PTT crystal unit cell are 4.64, 6.27, and 18.64 Å] (3) Two adjacent segments whose included angles are within 10 degrees are marked as mutually parallel. (4) A nucleus precursor is identified as a cluster containing mutually parallel segments. Based on this definition, we may easily determine the number n_s of nucleus precursors containing s parallel segments at any instant of time in the course of dynamic simulation. For example, the precursors identified from the NPT simulation at 400K are illustrated in Fig. 4 for 6 time instants. In the beginning of the simulation (e.g. 62 ps) most of the segments are disordered (in yellow). Several medium sized clusters (magenta, pink, red) start to form and some of them may continue to grow to a highly

oriented but loosely packed cluster (blue, after 1102 ps).

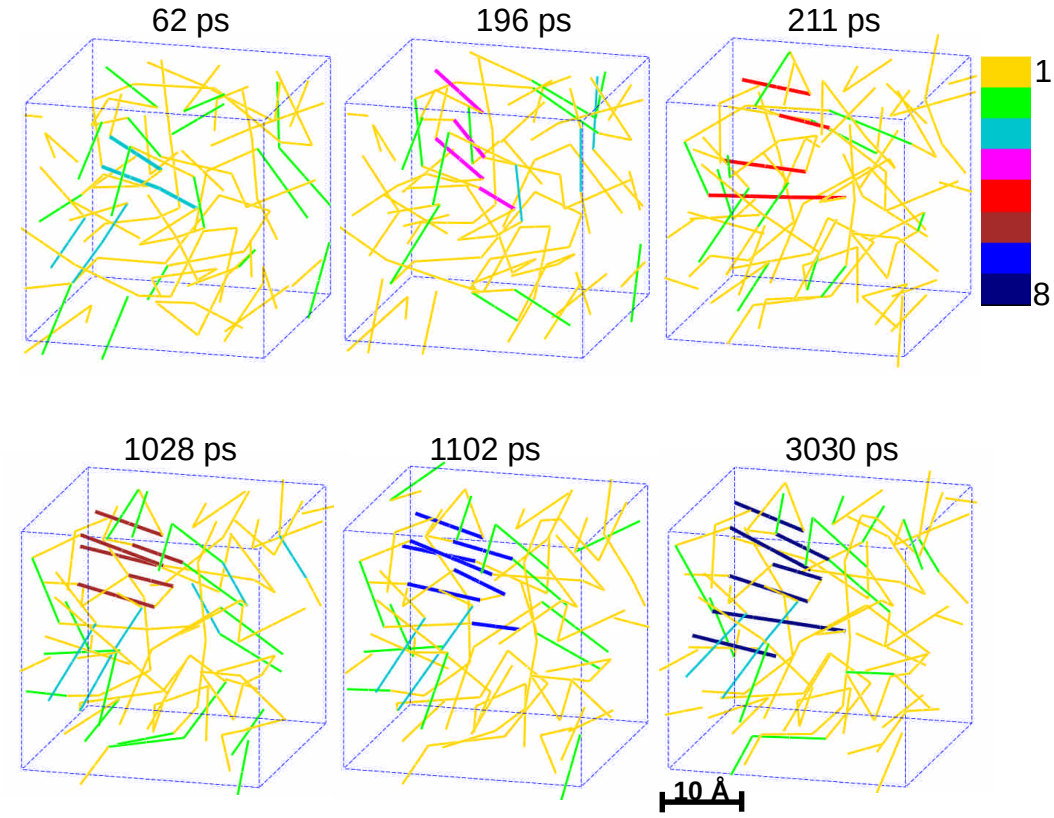

Figure 4. Illustration of the growth of nucleus precursor from melted state at 400 K. A color scale (from yellow (s=1) to dark blue (s=8)) is used for better discrimination of the size of precursors.

3.2 Growth of precursor

To quantify precursor development in the system, we define the average number $\langle n_s \rangle$ of appearance of precursors of size *s* as the average value of n_s (calculated at every picosecond) over one nanosecond. In Fig. 5 the time variation of $\langle n_s \rangle$ is depicted for s=3, 5, and 8 (other precursor sizes show similar behaviors) at temperatures from 50 K to 600 K. Small sized precursors (s=3,4,5) appears soon after the quenching process. (Note that we have excluded s=2 from the candidate of precursor because formation of such clusters highly depends on segment collisions and the value of $\langle n_2 \rangle$ is almost time invariant at a given temperature. This can also been seen from the green clusters in Fig. 4.) In addition, there is an increase of $\langle n_s \rangle$ with time at about 400 K but an decrease of $\langle n_s \rangle$ at temperatures near T_m and T_g. Little or no large precursors (s=6,7,8) were found in the beginning of simulation but they do emerge and grow, especially at around 400 K. As a consequence we observe the $\langle n_s \rangle$ for a certain sized precursor to have a maximum at 400 K.

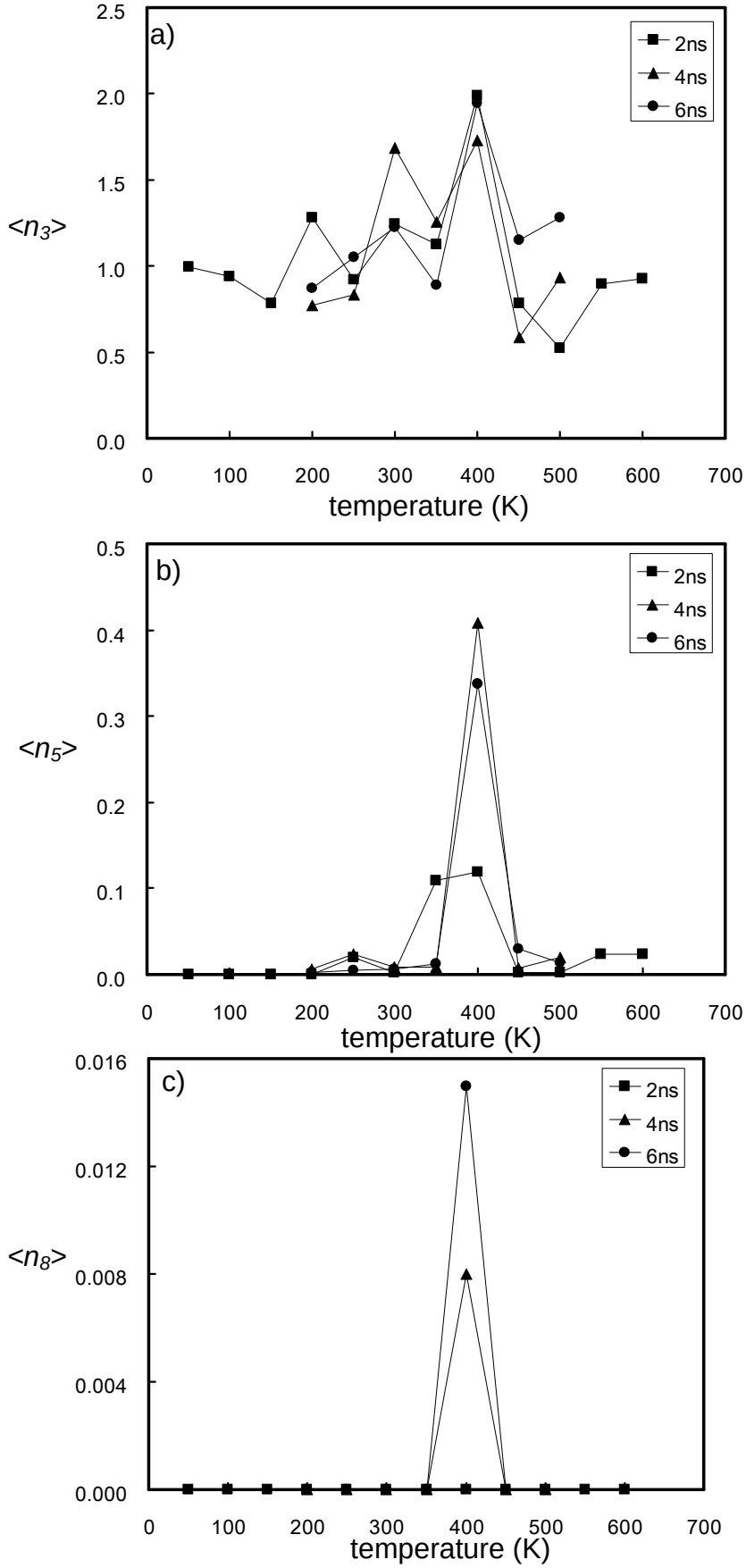

Figure 5. The variation of precursor number <n_s> with temperature at different times. (a) s=3, (b) s=5,.(c) s=8.

The development of precursors indicates the increase of local ordering within the system. Since their appearance is much earlier than the more compact nuclei, we refer this stage as precrystallization (induction period) and the local ordering as precrystallinity. (We have separately confirmed that the system as a whole remain isotropic at all temperatures, i.e., there is no long-ranged directional preference for the orientation of the precursors as one would expect from quenching.) To quantify the local ordering, we define the degree of precrystallinity X_s from precursors of size s as $X_s = s < n_s > /(\sum_{i=1}^{\infty} i < n_i >)$, and the total degree of precrystallinity X to be $X = \sum_{s=3}^{\infty} X_s$. From Fig. 6, one can observe a clear trend of enhancement of precrystallinity with time near temperature 400 K. Strikingly the temperature dependence of the pre-crystallinity curve resembles that of nucleation rate for common polymers. This indicates that the existence of nucleus precursors plays an important role in the nucleation process.

With a closer analysis of the simulation trajectory, we found that the formation and growth of nucleus precursors is a highly dynamical process. In the liquid state (600 K) there are constant formation and disintegration of small clusters (s=3,4,5) via segment vibration and collisions, i.e., these clusters are short-lived. As the system is quenched below T_m, some segments may agglomerate or deposit on a nearby cluster to form larger sized precursors. In the subsequent NPT runs, these precursors may grow, break down to small clusters, or dissolve back to the amorphous phase. Both the growth and disintegration of precursors are observed in this stage, however, the net effect (for a certain sized cluster to grow or dissolve) depends on the temperature and the size of the precursor (as it should be driven by thermodynamic equilibrium). As the temperature falls below T_g, small precursors become long-lived, however, most of them lose sufficient mobility to overcome barriers which prevents the formation and growth of larger precursors. As a consequence, we observe the presence of precursors peaks at a temperature between T_g and T_m.

Figure 7 shows the variation of X_s and X with time at 400 K, at which condition the growth rate of precursors is maximum from our simulation. It is seen that local ordering from small precursors reaches a steady value within 7 ns, while those from large precursor may continue to grow. By fitting $X(t)$ to the Avrami equation ($X(t) = X(t=\infty)\left[1-\exp(-kt^n)\right]$), we find that the the Avrami rate constant k is 8.16×10^7 s^{-n} (n = 0.9). This is quite rapid compared to the values 2.14×10^{-4} s^{-n} (n = 2.6) for primary nucleation and 1.15×10^{-1} s^{-n} (n = 0.8) for secondary nucleation from experiment at 450 K [4], at which condition the growth rate of PTT nuclei is maximum from experiment.

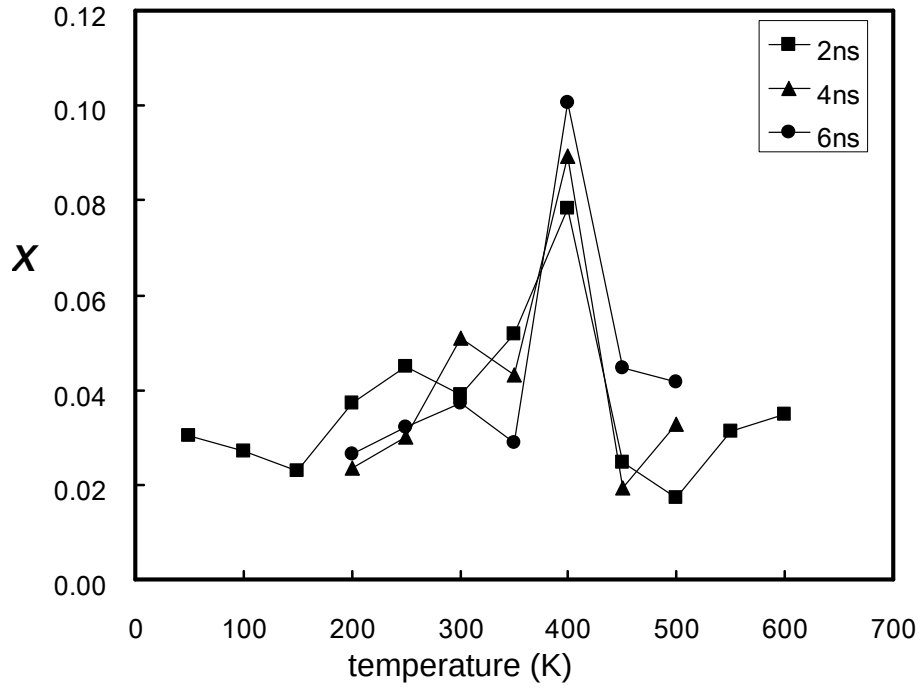

Figure 6. Variation of total precrystallinity with temperatures at different simulation times.

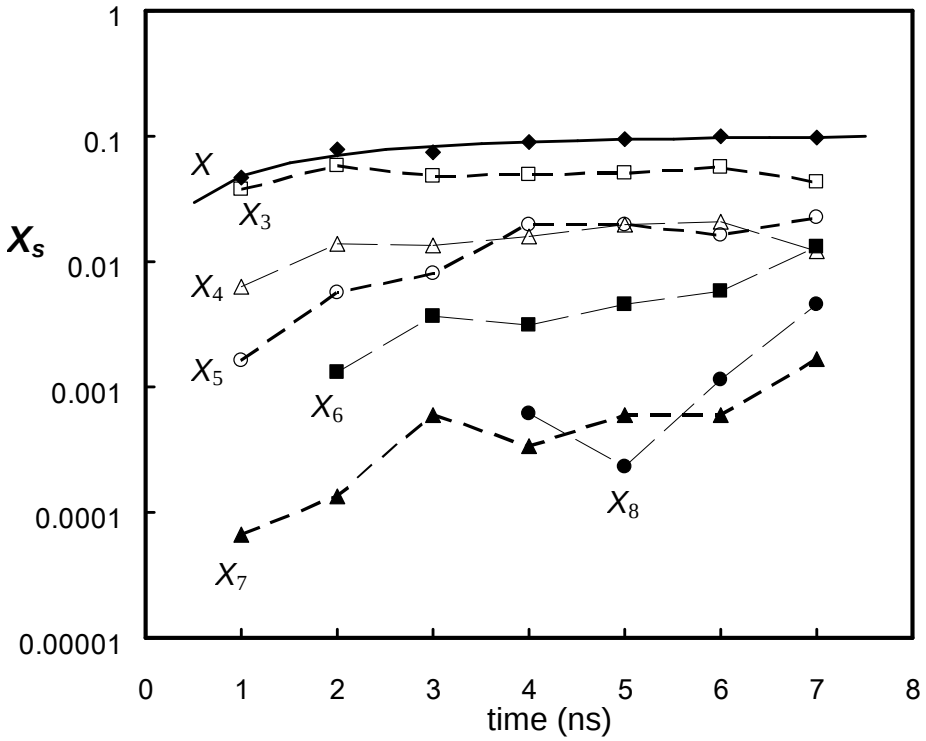

Figure 7. Time evolution of the precrystallinity X_s from s=3 to 8 and total precrystallinity X at 400K. The solid curve for X is the calculation based on the Avrami equation.

Future work (計畫成果自評)

We have observed the formation of nucleus precursors prior to the crystallization process. It is found that the growth rate of nucleus precursors has a remarkable resemblance to the nucleation rate of PTT. This indicates that the formation of precursor may assist in the nucleation process in the later stage. In the final year of this project, we will continue to investigate the nucleation process during cooling. In addition, we will study the process for PTT under stress. We will use the analysis tools developed over the past years to study the property-morphology relationships of PTT. The ongoing work include

1. Infrared analysis on PTT whiling cooling from the melt
2. investigation of the stress induced crystallization of PTT
3. investigation of the change of infrared spectrum during the crystallization of PTT
4. Establishment of the property-morphology relationships of PTT fibers

References

1. J.M. Huang and F.C. Chang, 2000, 38, *Crystallization kinetics of poly(trimethylene terephthalate).* Journal of Polymer Science Part B-Polymer Physics. p. 934-941.
2. X.S. Wang, D.Y. Yan, G.H. Tian, and X.G. Li, 2001, 41, *Effect of molecular weight on crystallization and melting of poly(trimethylene terephthalate). 1: Isothermal and dynamic crystallization.* Polymer Engineering and Science. p. 1655-1664.
3. P.D. Hong, W.T. Chuang, W.J. Yeh, and T.L. Lin, 2002, 43, *Effect of rigid amorphous phase on glass transition behavior of poly(trimethylene terephthalate).* Polymer. p. 6879-6886.
4. Y. Xu, S.R. Ye, J. Bian, and J.W. Qian, 2004, 39, *Crystallization kinetics analysis of poly(trimethylene terephthalate) including the secondary crystallization process.* Journal of Materials Science. p. 5551-5555.
5. M. Muthukumar, 2000, 3, *Commentary on theories of polymer crystallization.* European Physical Journal E. p. 199-202.
6. T. Yamamoto, 2005, 191, *Molecular dynamics modeling of the crystal-melt interfaces and the growth of chain folded lamellae.* Interphases and Mesophases in Polymer Crystallization III. p. 37-85.
7. P.D. Olmsted, W.C.K. Poon, T.C.B. McLeish, N.J. Terrill, and A.J. Ryan, 1998, 81, *Spinodal-assisted crystallization in polymer melts.* Physical Review Letters. p. 373-376.
8. G. Allegra and S.V. Meille, 1999, 1, *The bundle theory for polymer*

crystallisation. Physical Chemistry Chemical Physics. p. 5179-5188.

9. M. Soccio, A. Nogales, N. Lotti, A. Munari, and T.A. Ezquerra, 2007, 98, *Evidence of early stage precursors of polymer crystals by dielectric spectroscopy.* Physical Review Letters. p.
10. M. Imai, K. Kaji, T. Kanaya, and Y. Sakai, 1995, 52, *Ordering Process in the Induction Period of Crystallization of Poly(Ethylene-Terephthalate).* Physical Review B. p. 12696-12704.
11. E.L. Heeley, A.V. Maidens, P.D. Olmsted, W. Bras, I.P. Dolbnya, J.P.A. Fairclough, N.J. Terrill, and A.J. Ryan, 2003, 36, *Early stages of crystallization in isotactic polypropylene.* Macromolecules. p. 3656-3665.
12. G. Strobl, 2006, 31, *Crystallization and melting of bulk polymers: New observations, conclusions and a thermodynamic scheme.* Progress in Polymer Science. p. 398-442.
13. K. Fukao and Y. Miyamoto, 1997, 79, *Dynamical transition and crystallization of polymers.* Physical Review Letters. p. 4613-4616.
14. S. Sasaki, K. Tashiro, M. Kobayashi, Y. Izumi, and K. Kobayashi, 1999, 40, *Microscopically viewed structural change of PE during the isothermal crystallization from the melt - II. Conformational ordering and lamellar formation mechanism derived from the coupled interpretation of time-resolved SAXS and FTIR data.* Polymer. p. 7125-7135.
15. P. Panine, V. Urban, P. Boesecke, and T. Narayanan, 2003, 36, *Combined small- and wide-angle X-ray scattering study of early stages of polymer crystallization.* Journal of Applied Crystallography. p. 991-994.
16. Z.G. Wang, B.S. Hsiao, E.B. Sirota, P. Agarwal, and S. Srinivas, 2000, 33, *Probing the early stages of melt crystallization in polypropylene by simultaneous small- and wide-angle X-ray scattering and laser light scattering.* Macromolecules. p. 978-989.
17. H. Meyer and F. Muller-Plathe, 2002, 35, *Formation of chain-folded structures in supercooled polymer melts examined by MD simulations.* Macromolecules. p. 1241-1252.
18. J. Rieger, *Polymer crystallization : observations, concepts, and interpretations*, G. Reiter and J.U. Sommer, Editors. 2003, Berlin ; New York, Springer. p. 9~16.
19. R.H. Gee, N. Lacevic, and L.E. Fried, 2006, 5, *Atomistic simulations of spinodal phase separation preceding polymer crystallization.* Nature Materials. p. 39-43.
20. *Cerius*^{2}. 2003, Accelrys Inc.: San Diego.
21. J.E. Mark, ed. *Physical properties of polymers handbook.* 1996, AIP Press: Woodbury, N.Y.

22. S.S. Jang and W.H. Jo, 1999, 110, *Analysis of the mechanical behavior of poly(trimethylene terephthalate) in an amorphous state under uniaxial extension-compression condition through atomistic modeling.* Journal of Chemical Physics. p. 7524-7532.
23. S. Plimpton, 1995, 117, *Fast Parallel Algorithms for Short-Range Molecular-Dynamics.* Journal of Computational Physics. p. 1-19.
24. R.P. S. J. Plimpton, M. Stevens, . *Particle-Mesh Ewald and rRESPA for Parallel Molecular Dynamics Simulations*. in *Proc. of the Eighth SIAM Conference on Parallel Processing for Scientific Computing*. 1997. Minneapolis, MN.
25. J.L. Zhang, 2004, 91, *Study of poly(trimethylene terephthalate) as an engineering thermoplastics material.* Journal of Applied Polymer Science. p. 1657-1666.
26. R. Jakeways, I.M. Ward, M.A. Wilding, I.H. Hall, I.J. Desborough, and M.G. Pass, 1975, 13, *Crystal Deformation in Aromatic Polyesters.* Journal of Polymer Science Part B-Polymer Physics. p. 799-813.
27. I.M. Ward, M.A. Wilding, and H. Brody, 1976, 14, *Mechanical-Properties and Structure of Poly(Meta-Methylene Terephthalate) Fibers.* Journal of Polymer Science Part B-Polymer Physics. p. 263-274.
28. P.D. Hong, W.T. Chung, and C.F. Hsu, 2002, 43, *Crystallization kinetics and morphology of poly(trimethylene terephthalate).* Polymer. p. 3335-3343.

Appendix I

Publications from NSC supported projects.

1. **S.T. Lin** and C.M. Hsieh, "Efficient and accurate solvation energy calculation from polarizable continuum models", *Journal of Chemical Physics*, 125(12): an124103, 2006. (SCI,EI)

2. **S.T. Lin**, "Thermodynamic equations of state from molecular solvation", *Fluid Phase Equilibria*, 245(2): 185-192, 2006. (SCI,EI)

3. M.-T. Lee and **S.-T. Lin**, "Prediction of mixture vapor–liquid equilibrium from the combined use of Peng–Robinson equation of state and COSMO-SAC activity coefficient model through the Wong–Sandler mixing rule", Fluid Phase Equilibria, 254,28-34, 2007. (SCI,EI)

4. **S.T. Lin** and Y.-T. Tung, "Infrared spectroscopic analysis of poly(trimethylene terephthalate) from atomistic molecular dynamics simulations", *Polymer Preprint*, 2006.

Appendix III

Papers to be presented at the **AIChE 2007 Annual Meeting**, San Francisco, CA, September 10-14, 2006 in San Francisco (from 09-10-2006 to 09-14-2006)

Paper I: 01A09 Nucleation and Growth

Molecular Dynamic Simulations of Polymer Crystallization At The Early Stage

Min-Kang Hsieh and **Shiang-Tai Lin**, Department of Chemical Engineering, National Taiwan University, No. 1, Sec. 4, Roosevelt Road, Taipei, 10617, Taiwan

Our atomistic molecular dynamic simulations reveal the formation and growth of highly oriented but loosely packed clusters (nucleus precursors) upon quenching a melted semi-rigid polymer, poly(trimethylene terephthalate) (PTT). While extensive experimental and theoretical efforts are made to verify and explain the molecular mechanism in the growth of nuclei in polymeric materials, the primary stage of polymer crystallization is less well understood. Recent studies show that there exist nucleus precursors prior to the formation of crystal nuclei, and the simulation work of Gee et al. (2006) provided an unambiguous evidence of precursor formation as polymer melts are deep quenched into the unstable region where spinodal decomposition starts.

Here we show that such precursors may occur much earlier as soon as the polymer enters the metastable region. The temperature dependence of the local ordering (precrystallinity) caused by the formation of nucleus precursors resembles that of nucleation rate in common polymers. The growth of the precursor is found to be quite rapid, with the Avrami rate constant being, 8.16×10^{7} $s^{-0.9}$, and the precrystallinity

reaches about 10% at 400 K. Therefore the formation of the precursors is rather rapid and may play an important role as an incubator for crystal nuclei formation.

Paper II: 21000 Computational Molecular Science and Engineering Forum
Prediction Of Mixture Vapor-Liquid Equilibrium From The Peng-Robinson Equation Of State With Gex-Based Mixing Rule

Ming-Tsung Lee and **Shiang-Tai Lin**, Department of Chemical Engineering, National Taiwan University, No. 1, Sec. 4, Roosevelt Road, Taipei, 10617, Taiwan, Taipei, Taiwan

In this work we analyze the prediction of vapor-liquid equilibria (VLE) for a variety of binary mixtures over a wide range of temperature (183.15K – 623.15K) and pressure (0.1MPa -19 MPa) from the use of Peng–Robinson equation of state (PR EOS) and G^{ex}-based mixing rule, such as the Wong-Sandler (WS) and modified Huron-Vidal (MHV1) mixing rule. The predictive COSMO-SAC liquid activity coefficient model (LM) is used to provide the excess Gibbs free energy for the liquid phase.

In general, the predictions from the use of MHV1 mixing rule (average absolute error in pressure and in vapor phase composition are 2.5% and 4.9%, respectively) is more accurate than that from WS mixing rule (6.3%, 7.9%). It is found that the less accurate results from the WS mixing rule are owing to the inherent assumptions made. By means of analyzing excess energy, we found that the accuracy from the WS mixing rule can be improved with either of the two modifications: (1) The Stavermann –Guggenheim combinatorial term in the COSMO-SAC is ignored, and so the LM is denoted as $COSMOSAC^{res}$. The average error in both pressure and vapor phase composition from this approach is lowered to 4.0% and 4.7%, respectively. (2) Instead of matching G^{ex} from EOS and LM in the infinite pressure limit, we suggest to use the ambient condition instead. A detailed discussion for the improvements will be presented.